Article

Cation–Anion Interactions and Polar Structures in the Solid State

Michael R. Marvel, Julien Lesage, Jaewook Baek, P. Shiv Halasyamani, Charlotte L. Stern, and Kenneth R. Poeppelmeier

J. Am. Chem. Soc., **2007**, 129 (45), 13963-13969• DOI: 10.1021/ja074659h • Publication Date (Web): 18 October 2007

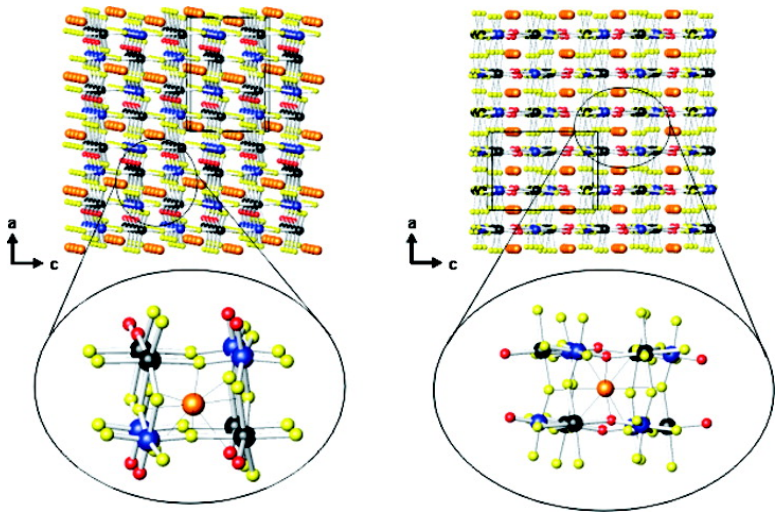

J|A|C|S
ARTICLES
Published on Web 10/18/2007

Cation−Anion Interactions and Polar Structures in the Solid State

Michael R. Marvel,[†] Julien Lesage,[†] Jaewook Baek,[‡] P. Shiv Halasyamani,[‡] Charlotte L. Stern,[†] and Kenneth R. Poeppelmeier*,[†]

Contribution from the Departments of Chemistry, Northwestern University, Evanston, Illinois 60208-3113, and University of Houston, 136 Fleming Building, Houston, Texas 77204-5003

Received June 25, 2007; E-mail: krp@northwestern.edu

Abstract: Complicated structures where oxygen and fluorine are found together in one framework, where deviations from Pauling's second crystal rule (PSCR) are expected, often result in structures with important physical properties. The $[NbOF_5]^{2-}$ anion and therefore all the individual Nb−O and Nb−F bonds are ordered in noncentrosymmetric $KNaNbOF_5$ and centrosymmetric $CsNaNbOF_5$. The Na/K− and Na/Cs−O/F interactions in these phases, in particular the expected deviations from PSCR and the bond valence model, reveal the essential role of the small potassium cations in the acentric packing of the $[NbOF_5]^{2-}$ anion. $KNaNbOF_5$ crystallizes in the orthorhombic and polar space group $Pna2_1$ (No. 33) with lattice constants a = 11.8653(11) Å, b = 5.8826(6) Å, c = 8.1258(8) Å, and Z = 4, while $CsNaNbOF_5$ crystallizes in the orthorhombic space group *Pbcn* (No. 60) with lattice constants a = 8.3155(7), b = 13.3176(11), c = 11.1314(9), and Z = 8.

Introduction

Noncentrosymmetric materials are a fertile topic of research owing to the important physical properties that may be observed in such materials: pyroelectricity, ferroelectricity, piezoelectricity, or second harmonic generation (SHG). Optimization of the latter property has been based largely on Chen's anionic group theory,[1] which attributes the SHG response in a material to the anionic group. This theory has proven useful by the continuous discovery of new NLO borates, for example, KBe_2BO_3F[2] and $Sr_2Be_2B_2O_7$.[3] While the design of SHG materials by selection of anionic groups that are able to produce high nonlinearities is a mostly successful method, it does not guarantee that one of the requirements for SHG materials, i.e., noncentrosymmetry, will be fulfilled.[4] In order to attain higher levels of predictability in designing noncentrosymmetric materials, the relationship between the anionic group and the surrounding bond network must also be understood. In this context, two compounds containing the acentric $[NbOF_5]^{2-}$ anion have been synthesized: noncentrosymmetric $KNaNbOF_5$ and centrosymmetric $CsNaNbOF_5$. This suggests that the noncentrosymmetric packing of the $[NbOF_5]^{2-}$ anion is related to the substitution of Cs^+ by the smaller K^+ cation in the $[NaNbOF_5]_\infty$ framework.

The $[NbOF_5]^{2-}$ anion is part of a large group of early d^0 transition metal oxide/fluoride octahedra: $[MO_xF_{6-x}]^{n-}$, with x = 1 for $M = V^{5+}$, Ta^{5+} (n = 2) and x = 2 for $M = Mo^{6+}$, W^{6+} (n = 2). Inherent to these anions are out-of-center "primary" electronic distortions that arise from metal dπ-oxygen pπ orbital interactions.[5] For example, the Nb atom moves from the center of the $[NbOF_5]^{2-}$ octahedron toward the oxide, forming a short Nb−O bond and a long *trans* Nb−F bond. This distortion is similar to that present in the technologically useful $LiNbO_3$ and $KTiOPO_4$ (KTP) materials. Other, secondary distortions are largely dependent on anion interactions with the extended bond network.

The first challenge one encounters in synthesizing a noncentrosymmetric material based on the $M^{V}OF_5^{2-}$ (M = V, Nb, Ta) or $M^{VI}O_2F_4^{2-}$ (M = Mo, W) anions is to prevent oxide/fluoride ligand disorder around the transition metal. The second is to prevent these anions from crystallizing in a centrosymmetric arrangement with respect to each other. The former, the challenge of O/F ordering, was overcome for all five anions and led to an analysis of their intraoctahedral distortions.[6] The latter, ordering in a noncentrosymmetric space group, was accomplished with the $[NbOF_5]^{2-}$ anion in inorganic−organic hybrid compounds but, surprisingly, never in an inorganic solid-state environment.

In inorganic−organic hybrid structures with cluster[7] and chain[8] motifs, the residual charge distribution on the oxide and fluoride ions bound to the M metal center dictates which specific cationic contacts are made to the oxide and fluoride ions. In general, the oxide and *trans*-fluoride ions of the $[NbOF_5]^{2-}$

[†] Northwestern University.
[‡] University of Houston.

(1) Ye, N.; Chen, Q.; Wu, B.; Chen, C. *J. Appl. Phys.* **1998**, *84*, 555−558.
(2) Wu, B.; Tang, D.; Ye, N.; Chen, C. *Opt. Mater. (Amsterdam)* **1996**, *5*, 105−109.
(3) Chen, C.; Wang, Y.; Wu, B.; Wu, K.; Zeng, W.; Yu, L. *Nature (London)* **1995**, *374*, 290.
(4) Becker, P. *Adv. Mater. (Weinheim, Ger.)* **1998**, *10*, 979−992.
(5) Kunz, M.; Brown, I. D. *J. Solid State Chem.* **1995**, *115*, 395−406.
(6) Welk, M. E.; Norquist, A. J.; Arnold, F. P.; Stern, C. L.; Poeppelmeier, K. R. *Inorg. Chem.* **2002**, *41*, 5119−5125.
(7) Heier, K. R.; Norquist, A. J.; Wilson, C. G.; Stern, C. L.; Poeppelmeier, K. R. *Inorg. Chem.* **1998**, *37*, 76−80.
(8) Norquist, A. J.; Heier, K. R.; Stern, C. L.; Poeppelmeier, K. R. *Inorg. Chem.* **1998**, *37*, 6495−6501.

10.1021/ja074659h CCC: $37.00

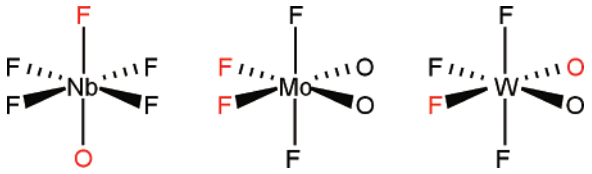

Figure 1. $[NbOF_5]^{2-}$, $[MoO_2F_4]^{2-}$, and $[WO_2F_4]^{2-}$ anions. The most nucleophilic O^{2-}/F^- ions are drawn in red. Coordination with the extended bond network takes place through these sites.

anion are the most reactive and preferentially coordinate to the extended bond network. Consequently, the $[NbOF_5]^{2-}$ anion is a *trans*-director. Similarly, one oxide ion and the fluoride ion *trans* to that oxide in $[WO_2F_4]^{2-}$ are the most nucleophilic.[9] In contrast, $[MoO_2F_4]^{2-}$ forms primary contacts through the two fluoride ions *trans* to the two oxide ions, and the anion is a *cis*-director (see Figure 1). Understanding these directional effects in early d^0 transition metal oxide/fluoride anions is essential in the design of new noncentrosymmetric materials.

The structure-directing role of octahedral oxide/fluoride anions in inorganic solids has not been elucidated because the anions typically crystallize with the oxide and fluoride ions disordered. As a step toward the construction of new solids with ordered oxide and fluoride ions, it has proven effective to create multiple solid-state contacts with different metal cations to the individual oxide and fluoride ions.[10,11] Pauling's second crystal rule (PSCR) states that, in a crystal structure, anions with the largest negative charges will occupy positions of the largest positive potential (bond strength).[12] This rule has been further quantified with the bond valence model, where the bond strengths are correlated to interatomic distances.[13] As a result, this principle is applicable only to compounds containing ordered oxide/fluoride anions of the early d^0 transition metals, where accurate bond lengths are obtained.

$KNaNbOF_5$ and $CsNaNbOF_5$ were targeted because the different alkali cations (K vs Na and Cs vs Na) should provide sufficiently different coordination environments to observe oxide and fluoride ordering.[14,15] Indeed, the six ions each reside on symmetry-unique positions, and each is coordinated to the extended bond network in a unique manner. Because the individual $[NbOF_5]^{2-}$ anions adopt a single orientation within the structure, accurate Nb−O and Nb−F bond lengths are obtained. Moreover, the $[NbOF_5]^{2-}$ anions in $KNaNbOF_5$ crystallize in a noncentrosymmetric arrangement with respect to each other. The crystal structure analyses presented here examine the underlying causes of oxide/fluoride ordering in these two compounds, the effects of the extended bond network on the observed primary and secondary distortions, and how changes to the bond network lead to different crystal symmetries.

Experimental

Caution: *Hydrofluoric acid is toxic and corrosive and must be handled with extreme caution and the appropriate protective gear! If contact with the liquid or vapor occurs, proper treatment procedures should be followed immediately.*[16−18]

Materials. Nb_2O_5 (99.9%, Aldrich), NaF (99.9%, Aldrich), KF (99.9%, Aldrich), RbF (99.9%, Aldrich), CsF (99.9%, Aldrich), and aqueous hydrofluoric acid (HF) (48% HF by weight, Aldrich) were used as received. Owing to their hygroscopic nature, the alkali fluorides were manipulated under nitrogen in a drybox.

Synthesis. All reactants were sealed in Teflon [fluoro(ethylenepropylene), FEP] "pouches".[19] The pouches were placed in a 125 mL Teflon-lined Parr pressure vessel filled 33% with deionized H_2O as backfill. The pressure vessel was heated for 24 h at 150 °C and cooled to room temperature over an additional 24 h. The pouches were opened in air, and the products were recovered by vacuum filtration.

$KNaNbOF_5$. $KNaNbOF_5$ was synthesized by reacting 0.0233 g (4.010×10^{-4} mol) of KF, 0.1000 g (4.010×10^{-4} mol) of Na_2NbOF_5 (see synthesis below), and 1.0 g (0.0555 mol) of deionized H_2O. Colorless plates were recovered in low yield. Increasing the amount of KF in the reaction vessel while holding all other starting materials constant led to the formation of $K_2NaNbO_2F_4$.[20] Decreasing the amount of KF in the reaction vessel led to the reprecipitation of Na_2NbOF_5. For further tests, polycrystalline $KNaNbOF_5$ was synthesized in 100% yield by solid-sate methods by reacting stoichiometric amounts of KF and $NaNbOF_4$ at 385 °C for 18 h under flowing argon.

$RbNaNbOF_5$. Polycrystalline $RbNaNbOF_5$ was synthesized in high yield by solid-state methods by reacting stoichiometric amounts of RbF and $NaNbOF_4$ (see synthesis below) at 385 °C for 18 h under flowing argon.

$CsNaNbOF_5$. $CsNaNbOF_5$ was synthesized by reacting 0.0608 g (4.002×10^{-4} mol) of CsF, 0.1344 g (0.0032 mol) of NaF, 0.4253 g (0.0016 mol) of Nb_2O_5, and 1.200 g (0.0600 mol) of 48% aqueous HF. Colorless needles were recovered in 80% yield based on Nb. Increasing the CsF:NaF ratio while holding all other starting materials constant led to the formation of cesium/niobium oxide/fluoride salts. Decreasing the CsF:NaF ratio while holding all other starting materials constant led to the formation of Na_2NbOF_5. Synthesis of large amounts of polycrystalline $CsNaNbOF_5$ by solid-state methods for further tests was not pursued because its centrosymmetric crystal structure precludes SHG, ferroelectric, and piezoelectric activity.

$NaNbOF_4$ and Na_2NbOF_5. $NaNbOF_4$ was synthesized by reacting 0.1344 g (0.0032 mol) of NaF, 0.4253 g (0.0016 mol) of Nb_2O_5, and 1.200 g (0.0600 mol) of 48% aqueous HF for approximately 2 h. A white polycrystalline powder was recovered in 88% yield based on Nb. Longer reaction times led to the destruction of the infinite chains of oxide-linked $(NbO_2F_4)_n$ octahedra and the formation of discrete $[NbOF_5]^{2-}$ units to give Na_2NbOF_5.[21]

Crystallographic Determination. Single-crystal X-ray diffraction data were collected with Mo Kα radiation ($\lambda = 0.71073$ Å) on a Bruker SMART-1000 CCD diffractometer and integrated with the SAINT-Plus program.[22] The structures were solved by direct methods and refined against F^2 by full-matrix least-squares techniques.[23] A face-indexed absorption correction was performed numerically using the program XPREP. The value of the Flack parameter[24] in $KNaNbOF_5$, estimated at 0.27(0.10), was then refined and converged at 0.28(0.11), but with no improvement of $R(F)$ (0.0420). The opposite configuration converged for a slightly higher $R(F)$ value of 0.0433. Although no definitive assignment of the absolute structure can be made, these results

(9) Heier, K. R.; Norquist, A. J.; Halasyamani, P. S.; Duarte, A.; Stern, C. L.; Poeppelmeier, K. R. *Inorg. Chem.* **1999**, *38*, 762−767.
(10) Needs, R. L.; Weller, M. T. *J. Chem. Soc., Chem. Commun.* **1995**, 353−354.
(11) Needs, R. L.; Weller, M. T. *J. Chem. Soc., Dalton Trans.* **1995**, 3015−3017.
(12) Pauling, L. *J. Am. Chem. Soc.* **1929**, *51*, 1010−1026.
(13) Brown, I. D.; Altermatt, D. *Acta Crystallogr., Sect. B* **1985**, *41*, 244−247.
(14) Welk, M. E.; Norquist, A. J.; Stern, C. L.; Poeppelmeier, K. R. *Inorg. Chem.* **2001**, *40*, 5479−5480.
(15) Antokhina, T. F.; Ignat'eva, L. N.; Savchenko, N. N.; Tkachenko, I. A.; Kaidalova, T. A. *Zh. Neorg. Khim.* **2003**, *48*, 551−558.
(16) Bertolini, J. C. *J. Emerg. Med.* **1992**, *10*, 163−168.
(17) Peters, D.; Miethchen, R. *J. Fluorine Chem.* **1996**, *79*, 161−165.
(18) Segal, E. B. *Chem. Health Saf.* **2000**, *7*, 18−23.
(19) Harrison, W. T. A.; Nenoff, T. M.; Gier, T. E.; Stucky, G. D. *Inorg. Chem.* **1993**, *32*, 2437−2441.
(20) Pausewang, G.; Ruedorff, W. *Z. Anorg. Allg. Chem.* **1969**, *364*, 69−87.
(21) Stomberg, R. *Acta Chem. Scand.* A **1984**, *38*, 603−607.
(22) *SAINT-Plus*, version 6.02A; Bruker Analytical X-ray Instruments, Inc.: Madison, WI, 2000.
(23) Sheldrick, G. M. *SHELXTL DOS/Windows/NT*, version 5.10; Bruker Analytical X-Ray Instruments, Inc.: Madison, WI, 1997.
(24) Flack, H. D. *Acta Crystallog., Sect. A* **1983**, *A39*, 876−881.

Table 1. Crystallographic Data for $CsNaNbOF_5$ and $KNaNbOF_5$

formula	$CsNaNbOF_5$	$KNaNbOF_5$
fw	359.81	266.01
space group	*Pbcn* (No. 60)	$Pna2_1$ (No. 33)
a (Å)	8.3155(7)	11.8653(11)
b (Å)	13.3176(11)	5.8826(6)
c (Å)	11.1314(9)	8.1258(8)
V (Å^3)	1232.7(7)	567.2(5)
Z	8	4
T (°C)	−120(1)	−120(1)
λ (Å)	0.71069	0.71069
ρ_{calc} (g/cm^3)	3.88	3.12
μ (mm^{-1})	7.86	2.95
$R(F)^a$	0.0266	0.0419
$wR_2(F^2)^b$	0.0680	0.1132
Flack parameter	n/a	0.27(0.10)

^{a} $R = \sum||F_o| - |F_c||/\sum|F_o|$. ^{b} $wR_2 = [\sum w(F_o^2 - F_c^2)^2/\sum w(F_o^2)^2]^{1/2}$.

indicate that the absolute configuration reported is likely correct. All structures were checked for missing symmetry elements with PLATON.[25] The final refinement includes anisotropic displacement parameters. Crystallographic data for $CsNaNbOF_5$ and $KNaNbOF_5$ are given in Table 1.

Second Harmonic Generation Measurement. A powder second-harmonic test was carried out on the $KNaNbOF_5$ sample by means of the Kurtz−Perry method.[26] About 100 mg of powder was hand-pressed into a pellet which was irradiated with a pulsed infrared beam (100 ns, 15 mJ, 10 Hz) produced by a Q-switched Nd:YAG laser of wavelength 1064 nm. A 532 nm filter was used to absorb the fundamental and pass the visible light onto a photomultiplier. A combination of a half-wave achromatic retarder and a polarizer was used to control the intensity of the incident power, which was measured with an identical photomultiplier connected to the same high-voltage source. This procedure was then repeated using a standard nonlinear optical material, in this case microcrystalline KH_2PO_4 (KDP), and the ratio of the second-harmonic intensity outputs was calculated. Since the SHG efficiency of powders has been shown to depend strongly on particle size,[26,27] polycrystalline $KNaNbOF_5$ was ground and sieved (Newark Wire Cloth Co.) into distinct particle size ranges (20−120 μm). To make relevant comparisons with known SHG materials, crystalline SiO_2 and $LiNbO_3$ were ground and sieved into the same particle size ranges. $KNaNbOF_5$, like $LiNbO_3$, was phase-matchable. The SHG response of $KNaNbOF_5$ was determined to be 0.6×KDP. Graphs of SHG responses vs particle sizes for $LiNbO_3$, α-SiO_2, and $KNaNbOF_5$ are available in the Supporting Information (Figure S1).

Results and Discussion

Extended Structures. Polyhedral representations of $KNaNbOF_5$ and $CsNaNbOF_5$ are shown in Figures 2 and 3. Individual six-coordinate Na, eight-coordinate K, and eight-coordinate Cs polyhedra are also shown. For the sake of comparison between the two structures, a maximum Cs−F bond distance of 3.40 Å has been chosen. However, the Cs1 and Cs2 coordination numbers can be increased to 10 and 12, respectively, if this value is fixed at 3.56 Å. Both the $KNaNbOF_5$ and $CsNaNbOF_5$ structures can be described as three-dimensional frameworks formed of (001) and (100) $[NaNbOF_7]_\infty$ layers stacked along *c* and *a*, respectively. The layers are composed of smaller $[NaNbO_2F_8]^{6-}$ building units that delineate four-sided windows, which stack to form channels. The K^+ and Cs^+ cations are located in these channels (see Figure 4).

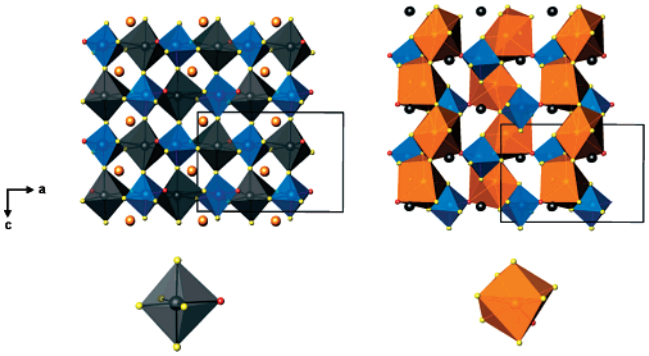

Figure 2. Coordination polyhedra in $KNaNbOF_5$. Blue octahedra are $[NbOF_5]^{2-}$ anions, black octahedra are Na-centered, and eight-coordinate orange polyhedra are K-centered. In this schematic, all drawings are shown in the (010) plane with different polyhedra highlighted in each.

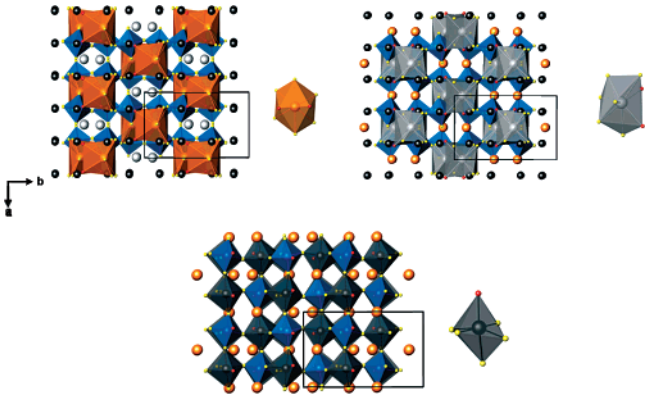

Figure 3. Coordination polyhedra in $CsNaNbOF_5$. Blue octahedra are $[NbOF_5]^{2-}$ anions, black octahedra are Na-centered, eight-coordinate orange polyhedra are Cs1-centered, and eight-coordinate gray polyhedra are Cs2-centered. In this schematic, all drawings are shown in the (001) plane with different polyhedra highlighted in each.

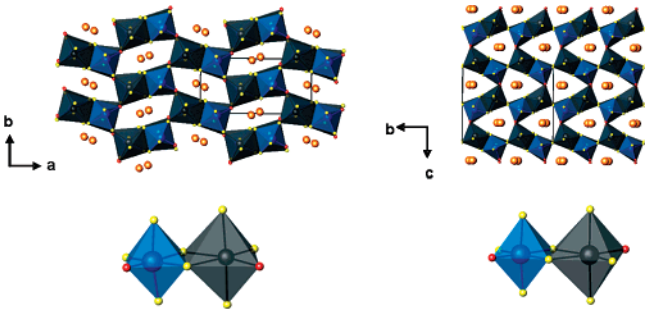

Figure 4. View of the three-dimensional frameworks in $KNaNbOF_5$ (left) and $CsNaNbOF_5$ (right), formed of (001) and (100) $[NaNbOF_7]_\infty$ layers stacked along *c* and *a*, respectively. Insets are views of the framework structural building unit.

In $KNaNbOF_5$, the Nb−O(1) bond length is 1.745(5) Å, while the *trans*-fluoride Nb−F(1) bond length is 2.114(4) Å. As expected, the Nb atom is located out of the plane formed by the equatorial fluorides, whose Nb−F distances range from 1.940(5) to 1.968(4) Å. In $CsNaNbOF_5$, the Nb−O(1) bond length is 1.800(3) Å and the *trans*-fluoride Nb−F(1) bond length is 2.056(2) Å, i.e., longer and shorter, respectively, than the corresponding bond lengths in $KNaNbOF_5$. The Nb atom, located out of the plane formed by the equatorial fluorides, forms four equatorial Nb−F bonds with distances that range from 1.930(2) to 1.955(2) Å. Selected bond distances are reported in Tables 2 and 3, with their associated experimental and theoretical bond valences and bond valence sums.

(25) Spek, A. L. *PLATON*; Utrecht University: Utrecht, The Netherlands, 2001.
(26) Kurtz, S. K.; Perry, T. T. *J. Appl. Phys.* **1968**, *39*, 3798−3813.
(27) Dougherty, J. P.; Kurtz, S. K. *J. Appl. Crystallogr.* **1976**, *9*, *Pt. 2*, 145−158.

Table 2. Selected Bond Lengths, Experimental Bond Valences, Theoretical Bond Valences, Bond Valence Sums, and BSI and GII Indices for $KNaNbOF_5$[a]

						$V_i = \sum_i S_{ij}$
		K		Na	Nb	$z_i = \sum_i s_{ij}$
O	R_{ij} (Å)	2.834(5)		2.343(6)	1.745(5)	
	S_{ij} (vu)	0.15		0.23	1.57	1.95
	s_{ij} (vu)	0.43		0.45	1.12	2.00
F1	R_{ij} (Å)	2.638(4)	2.726(4)	2.250(4)	2.114(4)	
	S_{ij} (vu)	0.17	0.14	0.21	0.52	1.04
	s_{ij} (vu)	0.07	0.07	0.10	0.76	1.00
F2	R_{ij} (Å)	2.732(2)		2.257(6)	1.946(4)	
	S_{ij} (vu)	0.14		0.21	0.81	1.16
	s_{ij} (vu)	0.10		0.12	0.79	1.00
F3	R_{ij} (Å)	2.700(4)	2.826(4)	2.446(5)	1.968(4)	
	S_{ij} (vu)	0.15	0.10	0.12	0.77	1.14
	s_{ij} (vu)	0.07	0.07	0.10	0.76	1.00
F4	R_{ij} (Å)	2.822(5)		2.297(8)	1.940(5)	
	S_{ij} (vu)	0.11		0.19	0.83	1.12
	s_{ij} (vu)	0.10		0.12	0.79	1.00
F5	R_{ij} (Å)	2.853(4)		2.205(5)	1.941(4)	
	S_{ij} (vu)	0.10		0.24	0.83	1.16
	s_{ij} (vu)	0.10		0.12	0.79	1.00
$V_j = \sum_j S_{ij}$		1.05		1.21	5.32	BSI = 0.15
$z_j = \sum_j s_{ij}$		1.00		1.00	5.00	GII = 0.16

[a] R_{ij}, bond length of the bond ij; $S_{ij} = \exp[(R_0 - R_{ij})/B]$, experimental bond valence, in valence units (vu), of bond ij, where R_0 is a constant dependent on i and j bonded elements, and $B = 0.37$ [R_0(Nb−O) = 1.911 Å, R_0(Nb−F) = 1.87 Å; R_0(Na−O) = 1.803 Å, R_0(Na−F) = 1.677 Å; R_0(Cs−O) = 2.417, R_0(Cs−F) = 2.33; R_0(K−O) = 2.132 Å, R_0(K−F) = 1.992 Å]; s_{ij}, theoretical bond valence, in valence units (vu), of bond ij, calculated by solving the network equations based on the methods described by Brown;[28,29] V_i, V_j, experimental valences of anions i and cations j; z_i, z_j, charge or formal valence of anions i and cations j; BSI = $[\langle(S_{ij} - s_{ij})^2\rangle]^{1/2}$, bond strain index; GII = $[\langle(V_{i,j} - z_{i,j})^2\rangle]^{1/2}$, global instability index.

Table 3. Selected Bond Lengths, Experimental Bond Valences, Theoretical Bond Valences, Bond Valence Sums, and BSI and GII Indices for $CsNaNbOF_5$[a]

						$V_i = \sum_i S_{ij}$
		Cs1	Cs2	Na	Nb	$z_i = \sum_i s_{ij}$
O	R_{ij} (Å)	2×3.247(3)	2×3.231(3)	2.300(3)	1.800(3)	
	S_{ij} (vu)	2×0.11	2×0.11	0.26	1.35	1.83
	s_{ij} (vu)	2×0.31	2×0.31	0.36	1.03	2.00
F1	R_{ij} (Å)	2×3.037(2)	2×2.964(2)	2.259(3)	2.056(2)	
	S_{ij} (vu)	2×0.15	2×0.18	0.21	0.60	1.14
	s_{ij} (vu)	2×0.06	2×0.06	0.11	0.78	1.00
F2	R_{ij} (Å)	2×3.202(2)		2.293(2)	1.941(2)	
	S_{ij} (vu)	2×0.10		0.19	0.82	1.11
	s_{ij} (vu)	2×0.08		0.13	0.79	1.00
F3	R_{ij} (Å)	2×3.110(2)	2×3.045(2)	2.401(3)	1.955(2)	
	S_{ij} (vu)	2×0.12	2×0.14	0.14	0.79	1.20
	s_{ij} (vu)	2×0.06	2×0.06	0.11	0.78	1.00
F4	R_{ij} (Å)			2.318(2)	1.946(2)	
	S_{ij} (vu)			0.18	0.81	0.99
	s_{ij} (vu)			0.17	0.83	1.00
F5	R_{ij} (Å)		2×3.335(2)	2.238(3)	1.930(2)	
	S_{ij} (vu)		2×0.07	0.22	0.85	1.14
	s_{ij} (vu)		2×0.08	0.13	0.79	1.00
$V_j = \sum_j S_{ij}$		0.94	1.00	1.20	5.24	BSI = 0.12
$z_j = \sum_j S_{ij}$		1.00	1.00	1.00	5.00	GII = 0.15

[a] See the Table 2 footnote for an explanation of the terms.

Based on powder X-ray diffraction data, $RbNaNbOF_5$ is isostructural with $CsNaNbOF_5$ (see Figure S2).

Anion Ordering and Observance of Pauling's Second Crystal Rule. The construction of noncentrosymmetric materials from early d^0 transition metal oxide/fluoride anions first requires that the oxide and fluoride ions crystallize without disorder. This is the case in both $KNaNbOF_5$ and $CsNaNbOF_5$. Oxide/fluoride order can be understood in the context of Pauling's second crystal rule, which states that anions with the largest negative potentials will occupy sites having the largest positive potentials. The assessment of the positive potential in the crystal frameworks, carried out by calculating the PSCR (bond strength) sum[30] and bond valence sum[13,31] around each anionic position, should match as closely as possible the assessment of the negative potentials of each oxide and fluoride ion (Tables 2−4). The central Nb atom has been excluded from the PCSR calculations since we are only interested in the oxide/fluoride interactions with the extended network.

Table 4. Estimations of the Negative Potentials of the Ions of the $(NbOF_5)^{2-}$ Anions and the Surrounding Positive Potentials in $CsNaNbOF_5$ and $KNaNbOF_5$, through Bond Strength and Bond Valence Calculations

bond	anionic BV (vu) [a]	cationic PSCR sum (vu) [b]	cationic BV sum (vu) [c]
	$CsNaNbOF_5$		
Nb−O	0.65	0.42	0.48
Nb−F1	0.40	0.42	0.54
Nb−F2	0.17	0.29	0.28
Nb−F3	0.21	0.42	0.40
Nb−F4	0.19	0.17	0.18
Nb−F5	0.15	0.29	0.29
	$KNaNbOF_5$		
Nb−O	0.43	0.29	0.38
Nb−F1	0.48	0.42	0.52
Nb−F2	0.19	0.29	0.33
Nb−F3	0.23	0.42	0.38
Nb−F4	0.17	0.29	0.30
Nb−F5	0.17	0.29	0.34

[a] Anionic bond valence (BV) = $z_i - S_{Nb-O/F}$, where z_i is the electric charge of each ligand and $S_{Nb-O/F}$ is taken from Table 2 or 3 for each Nb−O/F bond. [b] Cationic PSCR sum = $\sum_j s'_{j,cat} = \sum_j (z_{j,cat}/v_{j,cat})$, where $z_{j,cat}$ is the electric charge of each A_i alkali cation bonded to a given ligand and $v_{j,cat}$ is its coordination number. [c] Cationic bond valence (BV) sum = $\sum_i S_{i,cat}$, where $S_{i,cat}$ is taken from Table 2 or 3 for each A_i−O/F bond.

In inorganic−organic hybrid compounds that contain the $[NbOF_5]^{2-}$ anion, the anions connect to the extended network through the most charged oxide and fluoride ions. Similarly, in $KNaNbOF_5$, the F1 and F3 fluoride ions, which occupy positions in contact with two eight-coordinate K^+ cations and one six-coordinate Na^+ cation ($2 \times 1/8 + 1/6 = 0.42$ PSCR sum and bond valence sums of 0.52 and 0.38 vu, respectively), retain the most negative potentials (0.48 and 0.23 vu, respectively). The three remaining fluorides have less negative potentials: 0.19, 0.17, and 0.17 vu for F2, F4, and F5, respectively. They are each two-coordinate, with lower bond valence sums of 0.33, 0.30, and 0.34 vu, respectively, and PSCR sums of 0.29 (Table 4 and Figure 5). The same behavior is observed in $CsNaNbOF_5$, where the three-coordinate anionic sites are occupied by the three most nucleophilic ions (O1, F1, and F3), while F2, F4, and F5 are less reactive and are one- or two-coordinate (Table 4 and Figure 6).

(28) Brown, I. D. *The Chemical Bond in Inorganic Chemistry: The Bond Valence Model*, 1st ed.; Oxford University Press: Oxford, 2002; pp 240−243.
(29) Brown, I. D. *Phys. Chem. Miner.* **1987**, *15*, 30−34.
(30) Tobias, G.; Beltran-Porter, D.; Lebedev, O. I.; Van Tendeloo, G.; Rodriguez-Carvajal, J.; Fuertes, A. *Inorg. Chem.* **2004**, *43*, 8010−8017.
(31) Brese, N. E.; O'Keeffe, M. *Acta Crystallogr., Sect. B* **1991**, *47*, 192−197.

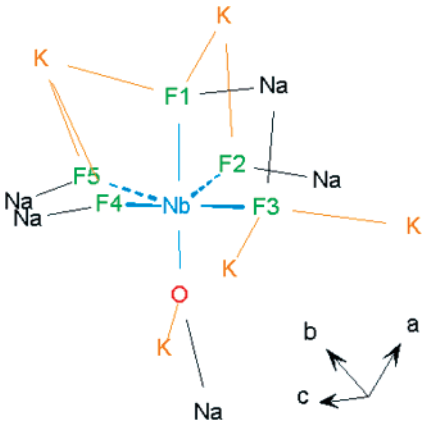

Figure 5. Asymmetric coordination environment surrounding the $[NbOF_5]^{2-}$ anion in $KNaNbOF_5$. The ions with the most local negative charge make the most/strongest contacts to the extended bond network.

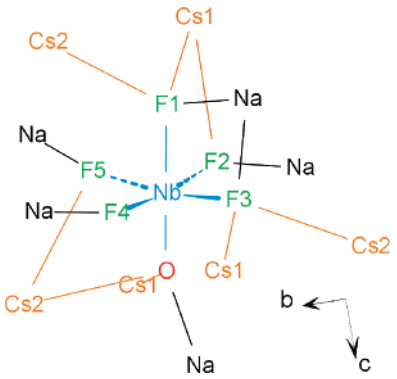

Figure 6. Asymmetric coordination environment surrounding the $[NbOF_5]^{2-}$ anion in $CsNaNbOF_5$. The ions with the most local negative charge make the most/strongest contacts to the extended bond network.

The observation that the O1 site in $KNaNbOF_5$ makes only two cationic contacts, in contrast to a high negative potential (0.43 vu), is understandable when other crystal chemical factors are considered. The polarizability of the oxide and fluoride ions also influences their interactions with the extended bond network. For instance, the "harder" (relative to oxide) F1 *trans*-fluoride interacts with three small, relatively nonpolarizable Na^+ (2.250(4) Å) and K^+ (2.638(4) and 2.726(4) Å) cations. At the same time, the central Nb atom displaces away from the *trans*-fluoride toward the "softer" oxide ion, which attracts only two cations, one Na^+ at 2.343(6) Å and one K^+ at 2.834(5) Å. In contrast, the oxide ion in $CsNaNbOF_5$ is three-coordinate, owing to the larger size of Cs^+.

Noncentrosymmetry versus Centrosymmetry. Oxide/fluoride ordering is only the first condition that must be met to engineer noncentrosymmetric materials with (V, Nb, or Ta)OF_5^{2-} or (Mo or W)$O_2F_4^{2-}$ anions. The anions must also crystallize in an acentric arrangement with respect to one another. Predictability in this second step can be achieved through an understanding of bond network−anion interactions.

Both $KNaNbOF_5$ and $CsNaNbOF_5$ contain channels that run along the length of the *b* axes. The K^+ cations move from the centers of the channels toward the *trans*-fluoride ligands (Table 2), the sites on the $[NbOF_5]^{2-}$ anions with the most negative electrostatic potential (Figure 7), resulting in a 2_1 screw axis along *c*. In contrast, the larger Cs^+ cations occupy inversion centers in the channel centers.

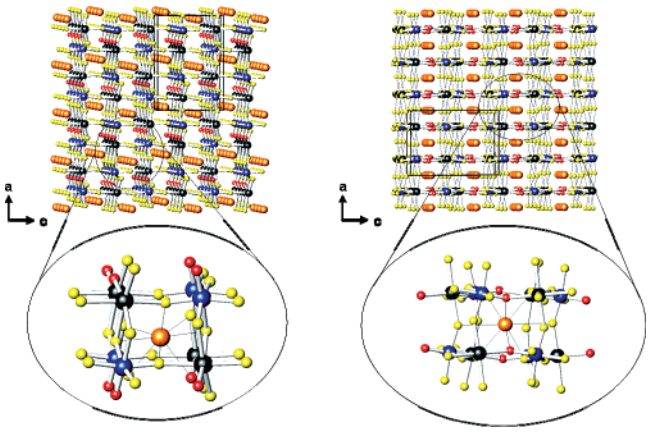

Figure 7. Channels formed by the Nb/Na−O/F framework, running along the length of the *b*-axis in $KNaNbOF_5$ (left) and $CsNaNbOF_5$ (right). Inset are enlarged views of the channel openings with cation coordination shown.

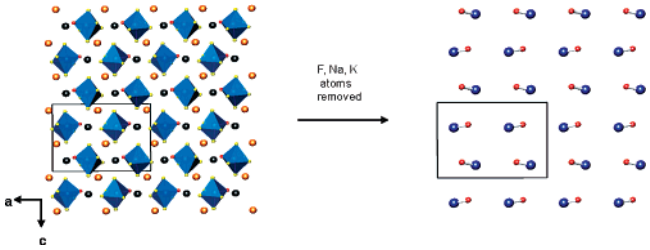

Figure 8. View of the primary Nb−O distortions in $KNaNbOF_5$ including all atoms (left) and only Nb and O atoms (right). The partial addition of the individual bond dipoles is enough to observe a significant SHG response (0.6×KDP).

Intraoctahedral Distortions and the Observed SHG Response in $KNaNbOF_5$. The complete alignment of dipole moments along the polar axis of a structure has been cited as the basis for highly efficient nonlinear optical materials, quantified by a structural parameter (*C*).[1] The polar distortion present in the $[NbOF_5]^{2-}$ anion is similar in magnitude to that of the NbO_6 octahedron in $LiNbO_3$.[32] However, the influence of bond networks is reported to play a role in altering the metal oxide/fluoride polyhedra from their idealized geometries.[6]

Both compounds exhibit primary, Nb−O distortions owing to crystallographic order of the octahedral anion. Centrosymmetry precludes the dipoles in $CsNaNbOF_5$ from summing in an additive manner. $KNaNbOF_5$ crystallizes in point group class *mm*2, and thus, though the individual bond dipoles do not align in an additive manner, they do not completely cancel each other (see Figure 8). The net polarity of $KNaNbOF_5$ leads to a fairly high SHG response (0.6×KDP). This value seems reasonable when it is considered that the NbO_6 octahedron is capable of producing SHG responses on the order of 13×KDP, as in $LiNbO_3$.[33] Similarly, in borates, a common group of SHG materials, partial cancellation of the second-order susceptibilities does not preclude the observation of a significant SHG response. For example, the BO_3 groups in the recently discovered $Li_6CuB_4O_{10}$ are oriented in opposite directions in alternating planes, yet an SHG response similar to that in KDP is observed.[34] In

(32) Maggard, P. A.; Nault, T. S.; Stern, C. L.; Poeppelmeier, K. R. *J. Solid State Chem.* **2003**, *175*, 27−33.
(33) Eaton, D. F. *Science (Washington, DC)* **1991**, *253*, 281−287.
(34) Pan, S.; Smit, J. P.; Watkins, B.; Marvel, M. R.; Stern, C. L.; Poeppelmeier, K. R. *J. Am. Chem. Soc.* **2006**, *128*, 11631−11634.

β-BaB_2O_4, the second-order susceptibility tensors cancel to a lesser extent, and an SHG response of 4×KDP is observed.[35]

Because the coordination sites of the bond network are asymmetrically arranged about the anion in both $KNaNbOF_5$ and $CsNaNbOF_5$, secondary distortions can be observed.[36] Unlike the primary, second-order Jahn−Teller distortions which are inherent to the $[MO_xF_{6-x}]^{2-}$ anions, these distortions arise from interactions between the extended three-dimensional bond network and the oxide and fluoride ions. When a ligand in a $[MO_xF_{6-x}]^{2-}$ anion interacts with its cationic environment, the M−O or M−F bond is weakened somewhat while its length increases to maintain its atomic valence, following the distortion theorem of the bond valence model. As a result, the central transition metal forms shorter, stronger bonds with the other oxide and fluoride ligands.[6,36]

The $[NbOF_5]^{2-}$ anion in $KNaNbOF_5$ exhibits a secondary distortion caused by electrostatic interactions with its cationic environment. Three cationic contacts are made to F3, while the remaining equatorial fluorides accept only two cationic contacts each (Table 2 and Figure 5). Consequently, the niobium−equatorial fluoride bond length, Nb−F3 (1.968(4) Å), is significantly larger than the remaining three (1.940(5), 1.941-(4), and 1.946(4) Å). The difference in Nb−equatorial fluoride bond lengths shows that, as the coordination number of an oxide or fluoride ion on the $[NbOF_5]^{2-}$ group increases, the strength of its interaction with the central Nb atom decreases. It is interesting to note in this context that M−O/F bond weakening also occurs in $Cs_2WO_2F_4$,[37] where each oxide or fluoride anion is surrounded by four equidistant cesium cations so that each ligand is in an identical coordination environment and the anion is disordered. In contrast, in $Na_2WO_2F_4$,[38] each oxide or fluoride ligand is coordinated by only two sodium cations and the anion retains W−O/F ordering.

The secondary distortion in $CsNaNbOF_5$ shares the same bond axis as the primary, Nb−O distortion. It is detectable, however, through comparison to the primary distortion in $KNaNbOF_5$. Tables 2 and 3 list the O^{2-}/F^- ions and their cationic interactions for $KNaNbOF_5$ and $CsNaNbOF_5$, respectively. Clearly, the $[NbOF_5]^{2-}$ anion is connected to the extended bond network in similar fashions: the fluoride *trans* to the oxide ligand and one equatorial fluoride accept three cationic contacts, while the remaining fluoride ions accept two or one (see Figures 5 and 6). The striking difference occurs at the oxide ions. The $KNaNbOF_5$ oxide ligand makes two cationic contacts, whereas the $CsNaNbOF_5$ oxide ligand makes three. As a result, the Nb−O bond in $CsNaNbOF_5$ (1.800(3) Å) is lengthened relative to the Nb−O bond in $KNaNbOF_5$ (1.744(5) Å). The difference in these two bond lengths can be taken as the lower limit of the magnitude of the secondary distortion in $CsNaNbOF_5$. The exact magnitude cannot be determined because a secondary distortion, though weaker, must also be present along the O−Nb−F axis in $KNaNbOF_5$ owing to an inequality in the strength of the interactions between the oxide and *trans*-fluoride ions. The observation that increasing the number of ionic contacts to the oxide ligand in a $[MO_xF_{6-x}]^{2-}$ anion leads to a decrease in the primary distortion of the anion agrees with previous computational work where it was shown that, as the number of bond network contacts made to the $[NbOF_5]^{2-}$ group increases, the steady weakening of the Nb−O interaction is due almost solely to a loss of π bonding.[39]

Analysis of Structural Strain. The primary electronic and secondary bond network-induced intraoctahedral distortions present in these compounds clearly cause deviations from PSCR which can be measured by determining the extent to which each structure violates the valence sum and equal valence rules. The valence sum rule[28] states that the sum of experimental bond valences around each atom is equal to the atomic valence, while the equal valence rule[28] states that the sum of bond valences around any loop in the bond network, with regard to the direction of the bond, is zero. These rules are collectively known as the network equations.[28] Their solutions, reported in Tables 2 and 3, are referred to as theoretical bond valences (s_{ij}). For example (see Table 2), the K^+ bonds to F1 and F3, and to F2, F4, and F5, have s_{ij} values of 0.07 and 0.10 vu, respectively, reflecting the fact that F1 and F3 are four-coordinate and F2, F4, and F5 are three-coordinate. Similarly, s_{ij} values for oxide bonds (K−O, Na−O, Nb−O) are greater than those for fluoride bonds owing to the oxide ion's higher negative charge. The ionic nature of the K−O and Na−O bonds accounts for the larger percentage the s_{K-O} (0.43 of 1.00) and s_{Na-O} (0.45 of 1.00) values contribute to the cation valence relative to the s_{Nb-O} value (1.12 of 5.00). The Nb^{5+} cation distributes its valence more equally among the ions in its coordination sphere.

Two indices have been proposed to measure the extent to which a structure violates the network equations. The global instability index (GII[40]) and bond strain index (BSI[41]) measure deviation from the valence sum rule and equal valence rule, respectively. A GII or BSI value greater than 0.05 vu indicates that a structure is strained, while a GII value greater than 0.20 vu indicates that a structure is unstable. The high values for both indices of $KNaNbOF_5$ and $CsNaNbOF_5$ indicate the structures are distorted. The BSI value for $KNaNbOF_5$ (BSI = 0.15) is significantly larger than that for $CsNaNbOF_5$ (BSI = 0.12), while the GII values are similar (0.16 and 0.15, respectively). The larger BSI and GII values for $KNaNbOF_5$ reflect the presence of primary and secondary distortions that are collectively greater in magnitude than those observed in $CsNaNbOF_5$. The stronger primary distortion observed in $KNaNbOF_5$ is also apparent in the higher theoretical bond valence of the Nb−O bond (1.12 vu) compared to that of the $CsNaNbOF_5$ Nb−O bond (1.03 vu). Increased cationic contact to the oxide ion clearly weakens the primary Nb−O distortion. Thus, it is observed that, in a series of compounds composed of the same basic building units, i.e., $[NbOF_5]^{2-}$ and alkali cations, the one that is noncentrosymmetric and polar has the greatest value of both the BSI and GII.

Conclusions

The interactions of the $[NbOF_5]^{2-}$ anion with the combination of Na/K or Na/Cs differ significantly. These lattice-derived

(35) Li, R.; Chen, C. *Wuli Xuebao* **1985**, *34*, 823−827.
(36) Izumi, H. K.; Kirsch, J. E.; Stern, C. L.; Poeppelmeier, K. R. *Inorg. Chem.* **2005**, *44*, 884−895.
(37) Srivastava, A. M.; Ackerman, J. F. *J. Solid State Chem.* **1992**, *98*, 144−150.
(38) Vlasse, M.; Moutou, J. M.; Cervera-Marzal, M.; Chaminade, J. P.; Hagenmuller, P. *Eur. J. Inorg. Chem.* **1982**, *19*, 58−64.
(39) Izumi, H. K.; Kirsch, J. E.; Stern, C. L.; Poeppelmeier, K. R. *Inorg. Chem.* **2005**, *44*, 884−895.
(40) Salinas-Sanchez, A.; Garcia-Munoz, J. L.; Rodriguez-Carvajal, J.; Saez-Puche, R.; Martinez, J. L. *J. Solid State Chem.* **1992**, *100*, 201−211.
(41) Preiser, C.; Losel, J.; Brown, I. D.; Kunz, M.; Skowron, A. *Acta Crystallogr., Sect. B: Struct. Sci.* **1999**, *B55*, 698−711.

secondary distortions, in addition to the primary electronic distortions they act upon, lead to a shorter Nb−O bond and oxygen being two-coordinate in the case of Na/K versus a longer Nb−O bond with oxygen three-coordinate for the combination Na/Cs. Thus, the noncentrosymmetric structure ($KNaNbOF_5$) maintains the larger primary electronic distortion of the $[NbOF_5]^{2-}$ anion along with a low coordination number of the electropositive K ion, consistent with the largest bond strain index (BSI). In contrast, the Cs ions of the centrosymmetric structure ($CsNaNbOF_5$) can exhibit significantly higher coordination numbers and the $[NbOF_5]^{2-}$ anion a greatly reduced primary distortion. Thus, structures that increase the number of cationic contacts to the oxide ion, which weaken the metal dπ-oxygen pπ interaction, are unlikely to result in noncentrosymmetric, polar structures.

Acknowledgment. The authors gratefully acknowledge support from the National Science Foundation (Solid State Chemistry Award Nos. DMR-0312136 and DMR-0604454) and the use of the Central Facilities, supported by the MRSEC program of the National Science Foundation (DMR-0076097 and DMR-0520513), at the Materials Research Center of Northwestern University. J.B. and P.S.H. thank the Texas Center for Superconductivity, the Welch Foundation, and the National Science Foundation (Grant DMR-0652150) for support.

Supporting Information Available: X-ray crystallographic files, in CIF format, including crystallographic details, atomic coordinates, anisotropic thermal parameters, and interatomic distances and angles, for $CsNaNaOF_5$ and $KNaNbOF_5$; SHG vs particle size curves for $LiNbO_3$, SiO_2, and $KNaNbOF_5$; indexed X-ray powder diffraction pattern for $RbNaNbOF_5$. This material is available free of charge via the Internet at http://pubs.acs.org.

JA074659H